STEADY THREE-DIMENSIONAL HYDROMAGNETIC STAGNATION POINT FLOW TOWARDS A STRETCHING SHEET WITH HEAT GENERATION

Hazem Ali Attia

Department of Engineering Mathematics and Physics
Faculty of Engineering
Fayoum University
Egypt

Abstract. An analysis is made of the steady hydromagnetic laminar three dimensional stagnation point flow of an incompressible viscous fluid impinging on a permeable stretching sheet with heat generation or absorption. A uniform magnetic field is applied normal to the plate which is maintained at a constant temperature. Numerical solution for the governing nonlinear momentum and energy equations is obtained. The effect of the strength of the uniform magnetic field, the surface stretching velocity, and the heat generation/absorption coefficient on both the flow and heat transfer is presented and discussed.

Introduction

The axisymmetric three-dimensional stagnation point flow was studied by Homann [1] who demonstrated that the Navier-Stokes equations governing the flow can be reduced to an ordinary differential equation of third order using similarity transformation. Later the problem of stagnation point flow either in the two- or three-dimensional cases [1], [2] has been extended in numerous ways to include various physical effects. The results of these studies are of great technical importance, for example in the prediction of skin-friction as well as heat/mass transfer near stagnation regions of bodies in high speed flows and also in the design of thrust bearings and radial diffusers, drag reduction, transpiration cooling and thermal oil recovery. In hydromagnetics, the problem of Hiemenz flow was chosen by Na [3] to illustrate the solution of a third-order boundary value problem using the technique of finite differences. An approximate solution of the same problem has been provided by Ariel [4]. The effect of an externally applied uniform magnetic field on the two or three-dimensional stagnation point flow was given, respectively, by Attia in [5] and [6] in the presence of uniform suction or injection. The study of heat transfer in boundary layer flows is of importance in many engineering applications such as the design of thrust bearings and radial diffusers, transpiration

cooling, drag reduction, thermal recovery of oil, etc. [7]. Massoudi and Ramezan [7] used a perturbation technique to solve for the stagnation point flow and heat transfer of a non-Newtonian fluid of second grade. Their analysis is valid only for small values of the parameter that determines the behavior of the non-Newtonian fluid. Later Massoudi and Ramezan [8] extended the problem to nonisothermal surface. Garg [9] improved the solution obtained by Massoudi [8] by computing numerically the flow characteristics for any value of the non-Newtonian parameter using a pseudo-similarity solution.

Flow of an incompressible viscous fluid over stretching surface has important applications in polymer industry. For instance, a number of technical processes concerning polymers involves the cooling of continuous strips (or filaments) extruded from a die by drawing them through a stagnant fluid with controlled cooling system and in the process of drawing these strips are sometimes stretched. The quality of the final product depends on the rate of heat transfer at the stretching surface. Crane [10] gave a similarity solution in closed analytical form for steady two-dimensional incompressible boundary layer flow caused by the stretching of a sheet which moves in its own plane with a velocity varying linearly with the distance from a fixed point. Carragher and Crane [11] investigated heat transfer in the above flow in the case when the temperature difference between the surface and the ambient fluid is proportional to a power of distance from the fixed point. Temperature distribution in the flow over a stretching surface subject to uniform heat flux was studied by Dutta et al. [12]. Recently, Chiam [13] analyzed steady two-dimensional stagnation-point flow of an incompressible viscous fluid towards a stretching surface. Temperature distribution in the steady plane stagnation-point flow of a viscous fluid towards a stretching surface was investigated by Ray Mahapatra and Gupta [14]. Steady flow of a non-Newtonian viscoelastic fluid [15]-[16] or micropolar fluid [17] past a stretching sheet was investigated with zero vertical velocity at the surface.

In the present paper the steady hydromagnetic laminar axisymmetric three dimensional stagnation point flow of an incompressible viscous fluid impinging on a permeable stretching surface is studied with heat generation/absorption. A uniform magnetic field directed normal to the plate is applied where the induced magnetic field is neglected [18]. The wall and stream temperatures are assumed to be constants. A numerical solution is obtained for the governing momentum and energy equations using finite difference approximations which takes into account the asymptotic boundary conditions. The numerical solution computes the flow and heat characteristics for the whole range of the uniform magnetic field, the surface stretching velocity, the heat generation/absorption coefficient and Prandtl number.

Formulation of the problem

Consider the steady three-dimensional stagnation point flow of a viscous incompressible fluid near a stagnation point at a surface coinciding with the plane $z = 0$, the flow being in a region $z > 0$. Two equal and opposing forces are applied along the radial direction so that the surface is stretched keeping the origin fixed. We use the cylindrical coordinates r, φ, z and assume that the wall is at $z = 0$, the stagnation point is at the origin and that the flow is in the direction of the negative z-axis. We denote the radial and axial velocity components in frictionless flow by U and W, respectively, whereas those in viscous flow will be denoted by $u = u(r, z)$ and $w = w(r, z)$ where the component in the φ direction vanishes [19]. A uniform magnetic field B_0 is applied normal to the plate where the induced magnetic field is neglected by assuming very small magnetic Reynolds number [18]. For three-dimensional flow let the fluid far from the plate, as z tends from infinity, be driven by the potential flow

$$U = ar, \quad W = -2az,$$

where a (> 0) is a constant characterizing the velocity of the mainstream flow. Then, from Euler equation the pressure distribution will be [19]

$$p = p_0 - \frac{\rho a^2}{2}\ (r^2 + 4z^2),$$

where ρ is the density of the fluid and p_0 is the pressure at the stagnation point. The continuity and momentum equations for the three dimensional steady state flows, using the usual boundary layer approximations [19], reduce to

$$(1) \quad \frac{\partial u}{\partial r} + \frac{u}{r} + \frac{\partial w}{\partial z} = 0,$$

$$(2) \quad \rho\left(u\,\frac{\partial u}{\partial r} + w\,\frac{\partial u}{\partial z}\right) = -\frac{\partial p}{\partial r} + \mu\left(\frac{\partial^2 u}{\partial r^2} + \frac{1}{r}\,\frac{\partial u}{\partial r} - \frac{u}{r^2} + \frac{\partial^2 u}{\partial z^2}\right) + \sigma B_0^2(U(r) - u),$$

$$(3) \quad \rho\left(u\,\frac{\partial w}{\partial r} + w\,\frac{\partial w}{\partial z}\right) = -\frac{\partial p}{\partial r} + \mu\left(\frac{\partial^2 w}{\partial r^2} + \frac{1}{r}\,\frac{\partial w}{\partial r} - \frac{u}{r^2} + \frac{\partial^2 w}{\partial z^2}\right),$$

where μ is the coefficient of viscosity of the fluid and σ is the electrical conductivity of the fluid. The boundary conditions for the above flow situation are

$$(4a) \quad z = 0 : u = cr,\ w = 0,$$

$$(4b) \quad z \to \infty : u \to ar,$$

where c is a positive constant related to the stretching velocity.

The boundary layer equations (1)-(3) admit a similarity solution

$$(5) \quad u = crf'(\eta),\ w = -2\sqrt{c\nu}\ f(\eta),\ \eta = \sqrt{c/\nu z},$$

where $\nu = \mu/\rho$ is the kinematic viscosity of the fluid and prime denotes differentiation with respect to η. If we now substitute u and w from Eq. (5) into the Navier-Stokes equations (1)-(3), we find that Eq. (3) yields simply the relation

$$\frac{\partial^2 p}{\partial r \partial z} = 0. \tag{6}$$

Using Eq. (5), Eqs. (1)-(2) and (4) lead to

$$f'^2 - f''' - 2ff'' - C^2 - Ha^2(C - f') = 0, \tag{7}$$

$$f(0) = 0,\ f'(0) = 1,\ f'(\infty) = C, \tag{8}$$

where $Ha^2 = \sigma B_0^2/c\rho$, Ha is the modified Hartmann number [18] and $C = a/c$ is the stretching parameter.

The governing boundary layer equation of energy, neglecting the dissipation, with temperature dependent heat generation or absorption is [19]

$$\rho c_p \left(u\ \frac{\partial \theta}{\partial r} + w\ \frac{\partial \theta}{\partial z} \right) = k\ \frac{\partial^2 T}{\partial z^2} + Q(T - T_\infty), \tag{9}$$

where θ is the temperature of the fluid, c_p is the specific heat capacity at constant pressure of the fluid, k is the thermal conductivity of the fluid, T_∞ the constant temperature of the fluid far away from the sheet, Q is the volumetric rate of heat generation/absorption, and T is the temperature profile. A similarity solution exists if the wall and stream temperatures, T_w and T_∞ are constants – a realistic approximation in typical stagnation point heat transfer problems [19].

The thermal boundary conditions are

$$z = 0 : T = T_w, \tag{10a}$$

$$z \to \infty : T \to T_\infty. \tag{10b}$$

By introducing the non-dimensional variable

$$\theta = \frac{T - T_\infty}{T_w - T_\infty},$$

and using Eq. (5), we find that Eqs. (9) and (10) reduce to,

$$\theta'' + 2\mathrm{Pr}\, f\theta' + \mathrm{Pr}\, B\theta = 0, \tag{11}$$

$$\theta(0) = 1,\ \theta(\infty) = 0, \tag{12}$$

where $\mathrm{Pr} = \mu c_p/k$ is the Prandtl number and $B = Q/c\rho c_p$ is the dimensionless heat generation/absorption coefficient.

The flow Eqs. (7) and (8) are decoupled from the energy Eqs. (11) and (12), and need to be solved before the latter can be solved. The flow Eq. (7)

constitutes a non-linear, non-homogeneous boundary value problem (BVP). In the absence of an analytical solution of a problem, a numerical solution is indeed an obvious and natural choice. The boundary value problem given by Eqs. (7) and (8) may be viewed as a prototype for numerous other situations which are similarly characterized by a boundary value problem having a third order differential equation with an asymptotic boundary condition at infinity. Therefore, its numerical solution merits attention from a practical point of view. The flow Eqs. (7) and (8) are solved numerically using finite difference approximations. A quasi-linearization technique is first applied to replace the non-linear terms at a linear stage, with the corrections incorporated in subsequent iterative steps until convergence. Then, Crank-Nicolson method is used to replace the different terms by their second order central difference approximations. An iterative scheme is used to solve the quasi-linearized system of difference equations. The solution for the Newtonian case is chosen as an initial guess and the iterations are continued till convergence within prescribed accuracy. Finally, the resulting block tri-diagonal system was solved using generalized Thomas' algorithm.

The energy Eq. (11) is a linear second order ordinary differential equation with variable coefficient, $f(\eta)$, which is known from the solution of the flow Eqs. (7) and (8) and the Prandtl number Pr is assumed constant. Equation (11) is solved numerically under the boundary condition (12) using central differences for the derivatives and Thomas' algorithm for the solution of the set of discritized equations. The resulting system of equations has to be solved in the infinite domain $0 < \eta < \infty$. A finite domain in the η-direction can be used instead with η chosen large enough to ensure that the solutions are not affected by imposing the asymptotic conditions at a finite distance. Grid-independence studies show that the computational domain $0 < \eta < \eta_\infty$ can be divided into intervals each is of uniform step size which equals 0.02. This reduces the number of points between $0 < \eta < \eta_\infty$ without sacrificing accuracy. The value $\eta_\infty = 10$ was found to be adequate for all the ranges of parameters studied here. Convergence is assumed when the ratio of every one of f, f', f'', or f''' for the last two approximations differed from unity by less than 10^{-5} at all values of η in $0 < \eta < \eta_\infty$.

Results and discussion

Figures 1 and 2 present the velocity profiles of f and f', respectively, for various values of C and Ha. The figures show that increasing the parameter C increases both f and f'. The effect of Ha on both f and f' depends on C. For $C < 1$, increasing Ha decreases f and f' while for $C > 1$, increasing Ha increases them. The figures indicate also that the effect of C on f and f' is more pronounced for smaller values of Ha. Also, increasing C decreases the velocity boundary layer thickness. Figure 3 presents the profile of temperature θ for various values of C and Ha and for $\mathrm{Pr} = 0.7$ and $B = 0.1$. It is clear that increasing C decreases θ and its effect on θ becomes more apparent for smaller values of Ha. The figure

indicates that the thermal boundary layer thickness decreases when C increases. Increasing Ha decreases θ for all C and its effect is more clear for smaller C.

Figure 4 presents the temperature profiles for various values of C and Pr and for $Ha = 1$ and $B = 0.1$. Figure 4 brings out clearly the effect of the Prandtl number on the thermal boundary layer thickness. As shown in Fig. 4, increasing Pr decreases the thermal boundary layer thickness for all C. Increasing C decreases θ and its effect is more apparent for smaller Pr. Figure 5 presents the temperature profiles for various values of C and B and for $Ha = 0.5$ and $\mathrm{Pr} = 0.7$. Increasing B increases the temperature θ and the boundary layer thickness. The effect of B on θ is more pronounced for smaller C. However, the effect of C on θ is more apparent for higher B.

Tables 1 and 2 present the variation of the dimensionless wall shear stress $f''(0)$ and the dimensionless heat transfer rate at the wall $-\theta'(0)$, respectively, for various values of C and Ha and for $\mathrm{Pr} = 0.7$ and $B = 0.1$. Increasing C increases $f''(0)$ for all Ha and its effect becomes more pronounced for higher Ha. Increasing Ha increases the magnitude of $f''(0)$ and its effect is more apparent for smaller C. It is of interest to see the reversal of the sign of $f''(0)$ for $C < 1$ for all Ha. Table 2 shows that, increasing C increases $-\theta'(0)$ for all Ha. The effect of C on $-\theta'(0)$ is more pronounced for higher Ha. For $C < 1$, increasing Ha decreases $-\theta'(0)$, however, for $C > 1$, increasing Ha increases $-\theta'(0)$.

Table 1. Variation of the wall shear stress $f''(0)$ with C and Ha

Ha	$C = 0.1$	$C = 0.2$	$C = 0.5$	$C = 1$	$C = 1.1$	$C = 1.2$	$C = 1.5$
0	−1.1246	−1.0556	−0.7534	0	0.1821	0.3735	1.0009
1	−1.4334	−1.3179	−0.9002	0	0.2070	0.4004	1.1157
2	−2.1138	−1.9080	−1.2456	0	0.2691	0.5445	1.4080
3	−2.9174	−2.6141	−1.6724	0	0.3494	0.7037	1.7954

Table 2. Variation of the wall heat transfer rate $-\theta'(0)$ with C and Ha ($\mathrm{Pr} = 0.7,\ B = 0.1$)

Ha	$C = 0.1$	$C = 0.2$	$C = 0.5$	$C = 1$	$C = 1.1$	$C = 1.2$	$C = 1.5$
0	0.6454	0.6819	0.7773	0.9109	0.9354	0.9588	1.0263
1	0.5974	0.6493	0.7653	0.9109	0.9365	0.9612	1.0309
2	0.5112	0.5901	0.7421	0.9109	0.9392	0.9661	1.0412
3	0.4402	0.5405	0.7211	0.9109	0.9419	0.9713	1.0522

Table 3 presents the effect of C on $-\theta'(0)$ for various values of Pr and for $Ha = 1$ and $B = 0.1$. Increasing C increases $-\theta'(0)$ for all Pr and its effect is more pronounced for higher Pr. Increasing Pr increases $-\theta'(0)$ for all C and its effect is more apparent for higher C. Table 4 presents the effect of the parameters

C and B on $-\theta'(0)$ for $Ha = 0.5$ and $\mathrm{Pr} = 0.7$. Increasing C increases $-\theta'(0)$ for all B. But, increasing B decreases $-\theta'(0)$ for all C.

Table 3. Variation of the wall heat transfer rate $-\theta'(0)$ with C and Pr ($Ha = 1$, $B = 0.1$)

Pr	$C = 0.1$	$C = 0.2$	$C = 0.5$	$C = 1$	$C = 1.1$	$C = 1.2$	$C = 1.5$
0.05	0.1273	0.1421	0.1845	0.2439	0.2545	0.2632	0.2919
0.1	0.1618	0.1911	0.2615	0.3343	0.3581	0.3700	0.4080
0.5	0.4691	0.5223	0.6345	0.7699	0.7933	0.8136	0.8793
1	0.7657	0.8152	0.9332	1.0888	1.1166	1.1408	1.2200

Table 4. Variation of the wall heat transfer rate $-\theta'(0)$ with C and B ($Ha = 0.5$, $\mathbf{Pr} = 0.7$)

B	$C = 0.1$	$C = 0.2$	$C = 0.5$	$C = 1$	$C = 1.1$	$C = 1.2$	$C = 1.5$
-0.1	0.1273	0.1421	0.1845	0.2439	0.2545	0.2632	0.2919
0	0.1618	0.1911	0.2615	0.3343	0.3581	0.3700	0.4080
0.1	0.4691	0.5223	0.6345	0.7699	0.7933	0.8136	0.8793

Conclusions

The three dimensional hydromagnetic stagnation point flow of a viscous incompressible fluid impinging on a permeable stretching surface is studied in the presence of uniform magnetic field with heat generation/absorption. A numerical solution for the governing equations is obtained which allows the computation of the flow and heat transfer characteristics for various values of the modified Hartmann number Ha, the stretching velocity, the heat generation/absorption parameter and the Prandtl number Pr. The results indicate that increasing the stretching velocity increases the velocity components but decreases the velocity boundary layer thickness. On the other hand, increasing the stretching velocity decreases the temperature as well as the thermal boundary layer thickness. The effect of the stretching parameter on the velocity and temperature is more apparent for smaller values of the magnetic field. The variation of velocity components as well as the rate of heat transfer at the wall with the magnetic field depends on the magnitude of the stretching velocity. The sign of the wall shear stress was shown to depend on the stretching velocity. The effect of the heat generation/absorption parameter B on the rate of heat transfer at the wall becomes more apparent for smaller C.

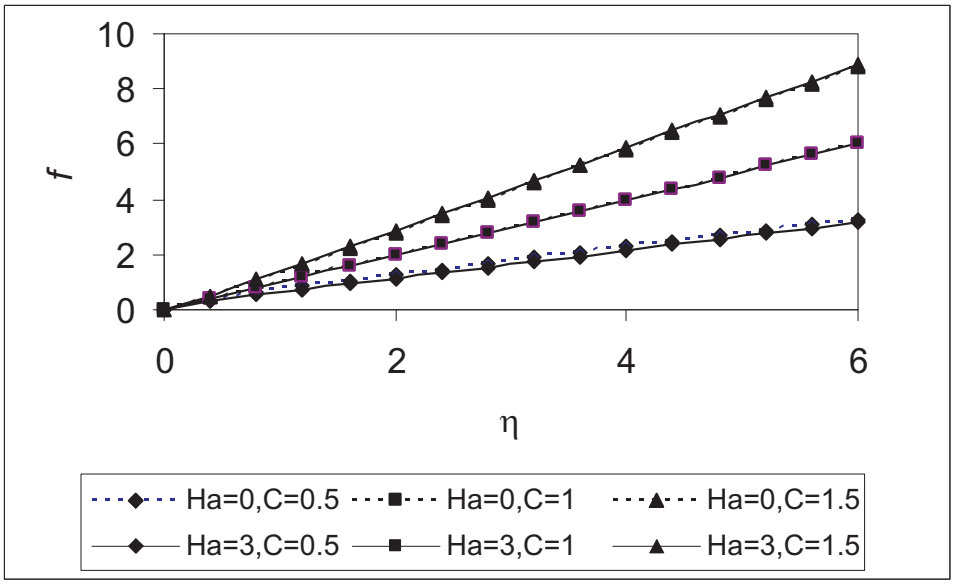

Figure 1: Effect of the parameters C and Ha on the profile of f

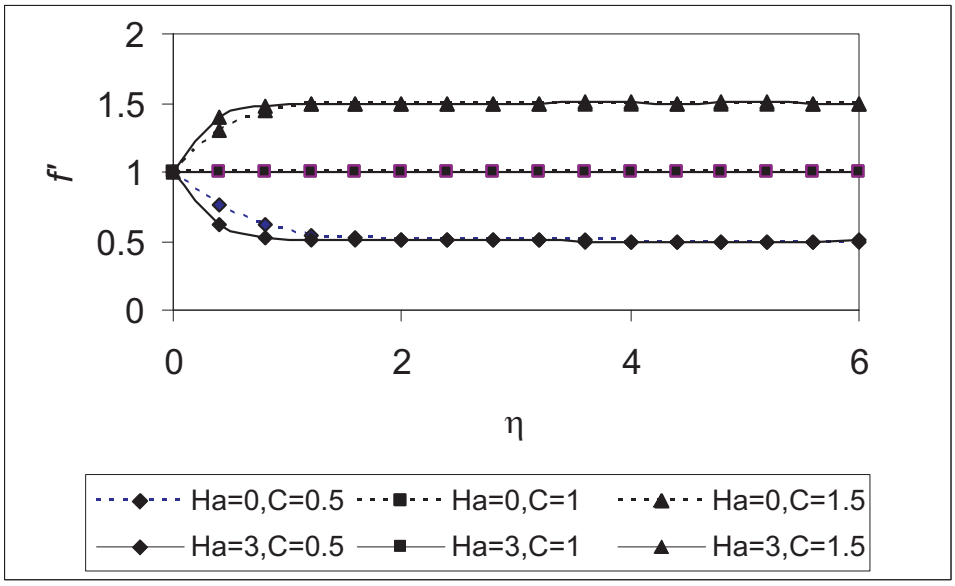

Figure 2: Effect of the parameters C and Ha on the profile of f'

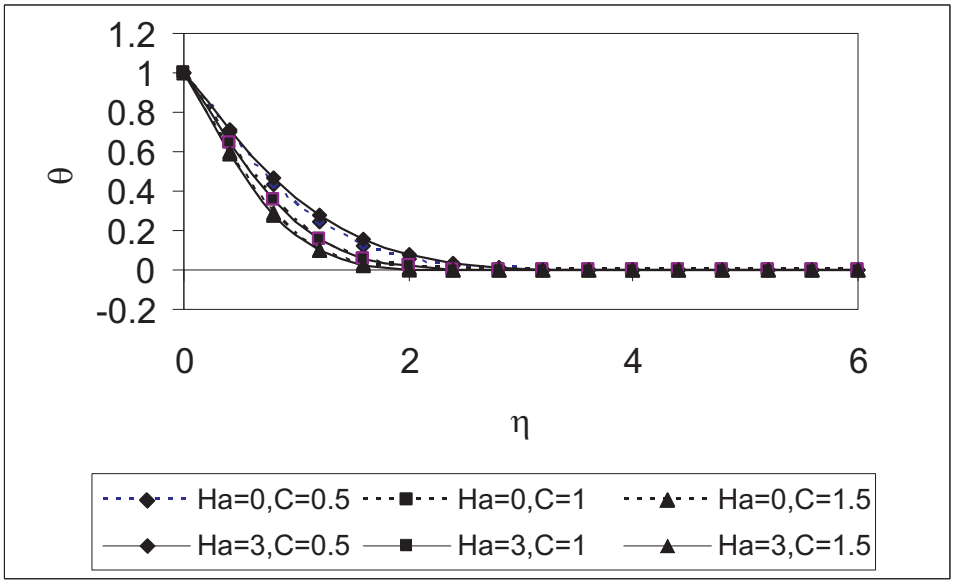

Figure 3: Effect of the parameters C and Ha on the profile of θ (Pr=0.7, B=0.1)

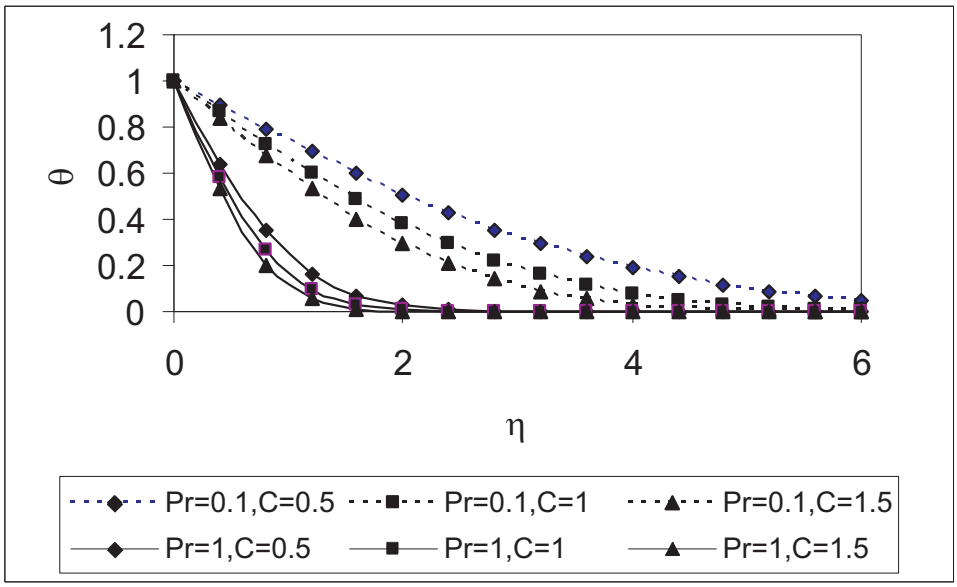

Figure 4: Effect of the parameters C and Pr on the profile of θ ($Ha = 1,\ B = 0.1$)

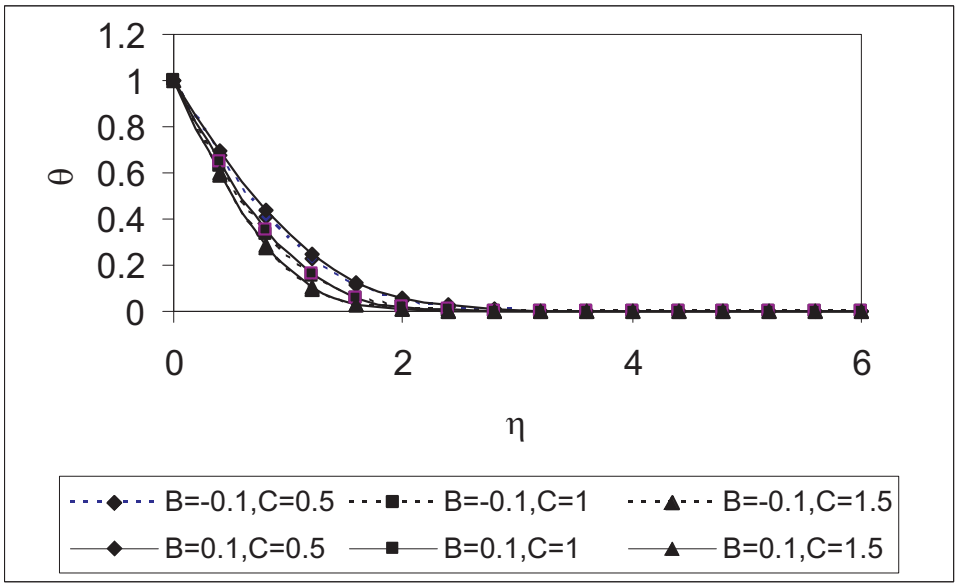

Figure 5: Effect of the parameters C and B on the profile of θ (Ha=0, 5, Pr=0.7)

References

[1] Homann, F., Z. Angew. Math. Mech., 16, 153 (1936).
[2] Hiemenz, K., Dingler Polytech. J., 326, 321 (1911).
[3] Na, T.Y., *Computational methods in engineering boundary value problem*, Academic Press, New York, 107 (1979).
[4] Ariel, P.D., Acta Mech., 103, 31 (1994).
[5] Attia, H.A., Arab. J. Sci. Engg. 28(1B), 107 (2003).
[6] Attia, H.A., Can. J. Phys., 81, 1223 (2003).
[7] Massoudi, M. and Ramezan. M., ASME HTD, 130, 81 (1990).
[8] Massoudi, M. and Ramezan. M., Mech. Res. Commun., 19 (2), 129 (1992).
[9] Garg, V.K., Acta Mech., 104, 159 (1994).
[10] Crane, L.J., ZAMP, 21, 645 (1970).
[11] Carragher, P., Crane, L.J., ZAMM, 62, 564 (1982).
[12] Dutta, B.K., Roy, P., Gupta, A.S., Int. Comm. Heat Mass Transfer, 12, 89 (1985).
[13] Chiam, T.C., J. Phys. Soc. Jpn., 63, 2443 (1994).
[14] Ray Mahapatra, T., Gupta, A.S., Heat Mass Transfer., 38, 517 (2002).
[15] Rajagopal, K.R., Na, T.Y., Gupta, A.S., Rheol. Acta., 23, 213 (1984).
[16] Ray Mahapatra, T., Gupta, A.S., Int.J. Nonlin. Mech., 39, 811(2004).
[17] Nazar, R., Amin, N., Filip, D., Pop, I., Int. J. Non-Linear Mech., 39, 1227 (2004).
[18] Sutton, G.W. and Sherman, A., *Engineering magnetohydrodynamics*, McGraw-Hill, New York, 1965.
[19] White, M.F., *Viscous fluid flow*, McGraw-Hill, New York, 1991.

Accepted: 29.09.2006